Food Quality and Safety, 2023, **7**, 1–14
https://doi.org/10.1093/fqsafe/fyad013
Advance access publication 23 February 2023
Article

OXFORD

Article

Malondialdehyde treatment reduced immunoreactivity of amandin and delayed its digestion

Xin Luo[1,2,3], Mingyan Ai[4], Yongyan Wu[1,2,3], Qia Wang[1,2,3], Hongbo Song[2], Qun Huang[2,3,5,6,*], and Jiankang Lu[1,*]

[1]Production & Construction Group Key Laboratory of Special Agricultural Products Further Processing in Southern Xinjiang, Tarim University, Ala'er, China
[2]College of Food Science, Fujian Agriculture and Forestry University, Fuzhou, China
[3]School of Public Health, The Key Laboratory of Environmental Pollution Monitoring and Disease Control, Ministry of Education, Guizhou Medical University, Guiyang, China
[4]Wuhan Academy of Agricultural Sciences, Wuhan, China
[5]Institute for Egg Science and Technology, School of Food and Biological Engineering, Chengdu University, Chengdu, China
[6]Key Laboratory of Endemic and Ethnic Diseases, Ministry of Education & Key Laboratory of Medical Molecular Biology of Guizhou Province, Guizhou Medical University, Guiyang, China

Correspondence to: Qun Huang, School of Public Health, Guizhou Medical University, Guiyang 550000, China. E-mail: huangqunlaoshi@126.com; Jiankang Lu, Production & Construction Group Key Laboratory of Special Agricultural Products Further Processing in Southern Xinjiang, Tarim University, Ala'er 843300, China. E-mail: lujiankang301@163.com

Abstract

Objectives: The secondary products of lipid oxidation are one of the main factors inducing protein oxidation. The effects of oxidation treatment with malondialdehyde (MDA) on the immunoreactivity of amandin and its digestion were studied.

Materials and Methods: The rabbit IgG binding ability of amandin was analyzed by western blotting, and the changes in amandin oxidation and immunoreactivity during digestion of amandin with different degrees of oxidation were investigated in combination with an almond allergen enzyme-linked immunosorbent assay kit. Alteration of linear epitopes of amandin by oxidation was investigated by liquid chromatography–tandem mass spectrometry (LC-MS/MS).

Results: The results showed that the immunoreactivity of amandin was significantly reduced after 1 mmol/L MDA and 100 mmol/L MDA treatment. However, the 1 mmol/L MDA treatment was owing to cleavage of linear epitope peptide in amandin and oxidation of the active amino acid. The 100 mmol/L MDA treatment was due to aggregation of amandin and significant decrease in its solubility. Oxidation also reduced digestibility of amandin and significantly affected immunoreactivity during digestion. LC-MS/MS also identified four oxidation-prone methionine sites (aa 264–274, 298–308, 220–240, and 275–297) in gamma conglutinin 1.

Conclusions: MDA treatment reduced the immunoreactivity of amandin. MDA treatment also led to protein aggregation, which slowed down the digestion of amandin and altered the immunoreactivity of amandin during digestion.

Keywords: Oxidation; amandin; immunoreactivity; digestion; LC-MS/MS.

Introduction

Almond is part of the tree nuts, which is one of the eight major groups of allergenic foods, and its allergies are long-lasting, serious, and even life-threatening. At present, there are seven almond allergens designated by the WHO/IUIS Allergen Nomenclature Committee. They are Pru du 3 (a non-specific lipid transfer protein 1), Pru du 4 (a profilin), Pru du 5 (60S acidic ribosomal protein 2), Pru du 6 (amandin), Pru du vicilin, Pru du 8 (an antimicrobial protein with cC3C repeats), and Pru du 10 (Zhang *et al.*, 2020; Costa and Mafra, 2022). Although vicilin and γ-conglutin were not designated by the WHO/IUIS Allergen Nomenclature Committee, they were confirmed to be food allergens. Almond pathogenesis related-10 protein, almond thaumatin-like protein and Pru du 2S albumin were considered food allergens due to their sequence homology with known food allergens.

Amandin, which was the major water-soluble protein in almonds, accounting for approximately 65% of soluble protein, was the allergenic protein in almonds containing the key peptide recognized by almond allergy sufferers (Tiwari *et al.*, 2010). Roux *et al.* (2001) and Zhang *et al.* (2013), respectively, developed an inhibitory enzyme-linked immunosorbent assay (ELISA) and a double-antibody sandwich ELISA, which provided a strong theoretical basis for the development and production of almond ELISA kits. In recent years, research on the immunoreactivity of almond protein has mainly focused on the influence of various factors in food technology. Zaffran *et al.* (2018) and Zhang *et al.* (2016) determined the IgE-binding capacity of amandin after heat treatment by ELISA.

Received 2 October 2022; Revised 27 January 2023; Editorial decision 30 January 2023

It was found that heat, pressure, and the synergy of water and pressure, such as dry heat at 400 °C, autoclaving (121 °C, 103 kPa, 30 min), and high-pressure treatment in the presence of water at 500 MPa, significantly reduced immunoreactivity. Other heat treatments, such as blanching, frying, and microwave heating, increased the immunoreactivity of amandin. Su *et al.* (2017) found that the immunoreactivity of amandin was relatively stable under different processing conditions.

Protein oxidation is also a non-negligible problem in food processing and storage. Oxidation not only changes the structure and physicochemical properties of proteins, but also affects the immunoreactivity of allergenic proteins. Huang *et al.* (2022) and Song *et al.* (2015) reported that malondialdehyde (MDA) treatment resulted in conformation changes in shrimp myosin, which further affected its IgE-binding capacity. 2,2′-Azobis (2-amidinopropane) dihydrochloride (AAPH) treatment could cause myosin aggregation and reduce the IgG/IgE-binding capacity (Lv *et al.*, 2019). Huang *et al.* (2017) found that the peptide separated from barley was cracked by metal catalytic oxidation, which significantly reduced immunoreactivity. Xin *et al.* (2022) studied the effects of oxidation on the structure and physicochemical properties of amandin. Gazme *et al.* (2022) found that although the gastrointestinal tract reduces the immunoreactivity of native egg white proteins, some of the IgE epitope-containing fragments remain intact during the digestion process. At present, the effect of MDA oxidation, a lipid oxidation product, on the immunoreactivity of amandin and changes in immunoreactivity during digestion have not been studied.

The indirect induction of lipid oxidation products was the main cause of protein oxidation, and MDA was the main secondary product of lipid oxidation. This paper mainly studies the changes in immunoreactivity of amandin after MDA treatment and the digestion process of amandin with different oxidation levels through western blotting analysis and almond ELISA kit. Liquid chromatography–tandem mass spectrometry (LC-MS/MS) was used to explore the changes in linear epitopes of amandin induced by oxidation, and to elucidate the mechanism of oxidative changes in amandin immunoreactivity. This provided us with a better understanding of the changes in amandin immunoreactivity caused by lipid peroxidation during food processing and storage.

Materials and Methods

Materials

The stone almonds were purchased from the almond farm in Shache County, Kashgar Prefecture (Xinjiang, China), and the harvest date was usually around 20 August. Almonds were harvested from the same variety and the same ripening period. Almond ELISA kit was purchased from Pribolab (Qingdao, China). All reagents and chemicals used in the experiment were analytically pure. All solutions are prepared with deionized water.

Amandin extraction

The extraction of amandin was performed according to the method of previous research (Xin *et al.*, 2022). The peeled almonds were crushed by a pulverizer (YF-150B, Yongli Pharmaceutical Machinery Co., Wenzhou, China). Oil in almond powder was extracted with anhydrous ether at 45°C with Soxhlet extraction, dried at room temperature (RT, approximately 25 °C), and refrigerated at −20 °C. Almond powder was extracted with 0.02% sodium azide distilled water by magnetic stirring (ZWYR-240, Shanghai Zhicheng Analytical Instrument Manufacturing Co., Ltd., Shanghai, China) at RT for 1 h. The mixture after extraction was centrifuged at 8000×*g* and 4 °C (TGL-16, Sichuan Shuke Instrument Co. Ltd., Chengdu, China) for 10 min, and the above extraction operation was repeated. The supernatant was filtered through a Belleofer funnel and then incubated at 4 °C overnight. The supernatant after standing was centrifuged for 20 min, and the precipitate was lyophilized and stored in a refrigerator at −20 °C for later use.

Amandin oxidation

The oxidation of amandin was performed according to the method of Lv *et al.* (2017) with slight modifications. MDA was obtained by hydrolysis of 1,1,3,3-tetramethoxypropane in 5.0 mol/L HCl at 40 °C for 30 min (pH 7.4) (PB-10, Sartorius Scientific Instruments Co. Ltd., Beijing, China). The absorbance of the diluted MDA was read at 267 nm by ultraviolet-visible spectrophotometer (UV-1780PC, Shimadzu Co. Ltd., Suzhou, China). MDA concentration was determined by molar extinction coefficient (31 500 mol^{-1} cm^{-1}).

MDA solution was mixed with amandin solution, and the final concentrations of MDA were 0, 0.01, 0.1, 1, 10, and 100 mmol/L. Then, the reaction was carried out under closed dark condition (25 °C) for 24 h. After the oxidation reaction, the reaction solution was placed in ice water to rapidly reduce the temperature to below 4 °C, and then it was dialyzed for 72 h. Finally, amandin oxidized by MDA was freeze-dried (FDU-1200, Shanghai Alang Instrument Co., Ltd., Shanghai, China) and stored at −20 °C for later use.

Determination of solubility

The solubility was measured according to the method of Luo *et al.* (2022). The protein solution was centrifuged at 10 000×*g* for 15 min at 4 °C. The protein concentration of the solution was measured before and after centrifugation. Solubility (%) represented the percentage of the protein content dissolved in solution to total protein content.

In vitro gastroduodenal digestion

Simulated gastric fluid (SGF) and simulated intestinal fluid (SIF) were prepared according to the United States Pharmacopoeia (Liu *et al.*, 2015). Simulated digestion *in vitro* of amandin followed the method of Toomer *et al.* (2013) with appropriate modifications. The SGF (pH 2.0, containing 2500 U/mg pepsin) was incubated in a water bath (DF-101S, Gongyi Yuhua Instrument Co., Ltd., Zhengzhou, China) at 37 °C for 10 min, and then amandin (10 mg/mL) was added to the SGF. The digestion times were 0, 0.5, 5, 10, 30, 60, 90, and 120 min, and 1 mol/L NaOH was added to stop pepsin digestion. After the digestion of SGF, SIF (pH 7.5) was added at a ratio of 1:1 (volume fraction). The digestion times were 0, 0.5, 10, 30, 60, and 90 min. Then the digested samples were heated in a boiling water bath for 10 min to deactivate the enzyme for subsequent analysis.

Sodium dodecyl sulfate–polyacrylamide gel electrophoresis

Sodium dodecyl sulfate–polyacrylamide gel electrophoresis (SDS-PAGE) was determined by referring to Huang *et al.*

(2021b) with Wang *et al.* (2021) and modified slightly. The amandin solution (8 mg/mL) was mixed with 4× sample loading buffer (containing β-mercaptoethanol; 3:1 (volume fraction)) and boiled for 10 min. The samples were cooled to RT and centrifuged (4 °C, 10 000×*g*, 10 min). Approximately 5 μL of supernatant was added to the gel (12% for separated gel and 5% for concentrated gel) and electrophoresis was performed at 100 V. The gel was dyed with Coomassie bright blue and decolorized until the strip was clear.

Western blotting

The determination method of western blotting was modified according to the method of Lv *et al.* (2019). The target region on the protein glue was cut off and soaked in methanol for 5 min before being transferred to the membrane transfer solution. The filter paper was laid flat on the sponge, and the sequence from the negative electrode to the positive electrode was: four layers of filter paper, glue, PVDF membrane, and four layers of filter paper. After sealing, it was transferred to a trans-blot and run for 1.5 h at 150 mA. The PVDF membrane was immersed in the sealing solution (approximately 2.5 g of skim milk powder was added to 50 mL of freshly prepared TBST (1% Tris–HCl, 0.9% NaCl, 0.05% Tween 20) solution with shaking) and blocking agent, and slowly rocked at RT for 60 min. Then the PVDF membrane was soaked in primary antibody and incubated at RT for 60 min or overnight at 4 °C. After primary antibody incubation (IgG rabbit sera), the PVDF membrane was washed with TBST five times. The PVDF membrane was infiltrated in the secondary antibody (horse radish peroxidase (HRP)-labeled goat anti-rabbit IgG) and incubated gently at RT for 60 min. After five washes with TBST, the horseradish peroxidase HRP-ECL luminescence method was used, and the images were taken in a chemiluminescence imaging analyzer.

Almond ELISA kit

The almond ELISA kit was used for the experiment. The 100 μL sample solution was added to the plate and incubated at RT for 20 min. The plate was washed three times with a concentrated wash buffer to remove unbound material. Approximately 100 μL of enzyme-labeled conjugate was added to the plate and incubated at RT for 20 min. Then, the plate was washed again. The substrate solution was added to avoid light reaction at RT for 20 min, and then the stop solution was added. The absorbance was measured at 450 nm.

LC-MS/MS

LC-MS/MS was performed according to the method described by Liu *et al.* (2021a) and Yang *et al.* (2020) with appropriate modifications. The peptide sample was redissolved. Nano-HPLC system UltiMate 3000 RSLCnano (Thermo Fisher Scientific, Waltham, MA, USA) was used for separation. Liquid A was 0.1% formic acid–aqueous solution, and liquid B was 0.1% formic acid–acetonitrile solution. The trap column was 100 μm×20 mm (RP-C18, Agilent) balanced with 100% solution A at 3 μL/min. The samples were loaded by an automatic sampler, combined to a trap column, and separated on an analysis column at a flow rate of 300 nL/min on a 75 μm×150 mm (RP-C18, New Objective, Littleton, MA, USA) column. The samples were cleaned by mobile phase gradient with blank solvent for 30 min. The hydrolysates were separated by capillary high performabce liquid chromatography (HPLC) and analyzed by Q-EXactive Plus mass spectrometry.

The scanning range of the parent ion was 300–1500 *m/z*, and the scanning mode of mass spectrometry was Data Dependent Acquisition (DDA). The 20 strongest fragments (MS2 Scan) are collected after each full scan. The fragmentation mode was as follows: High-energy Collision dissociation (HCD), NCE energy 28, dynamic exclusion time: 25 s. MS1 at *m/z* 200 had a resolution of 70 000, AGC target was set to $3e^6$, and the maximum injection time was 100 ms. MS2 had a resolution of 17 500, AGC target was set to $1e^5$, and the maximum injection time was 50 ms.

Statistical analysis

The test results were expressed as mean±standard deviation, and the number of sample replicates n=3. The different letters (a, b) indicated significant differences (P<0.05) between samples. SPSS software (Version 25.0.0; SPSS Inc., Chicago, IL, USA) was used for one-way analysis of variance (ANOVA). Differences between pairs of means were evaluated by Duncan's new multiple range test using a 95% confidence interval. All the curves in this paper were plotted using Origin 2018 (OriginLab, Northampton, MA, USA).

Results and Discussion

Solubility

Solubility could be used to evaluate the degree of aggregation of proteins, which would affect the functional properties of proteins (Huang, *et al.*, 2021a). Figure 1 shows the effect of oxidation on the solubility of amandin. Approximately 0.01–10 mmol/L MDA had no significant effect on the solubility of amandin. When the MDA concentration reached 100 mmol/L, the solubility of amandin decreased from 81.85% to 76.56% (P<0.05). Zhou *et al.* (2019) showed that the solubility of rice bran protein also decreased gradually with the increase of oxidation degree. This trend was consistent with the results of this study. Reactive oxygen species (ROS), such as peroxy radical and MDA, might cause proteins to form insoluble aggregates, which resulted in decreased solubility (Li *et al.* 2021).

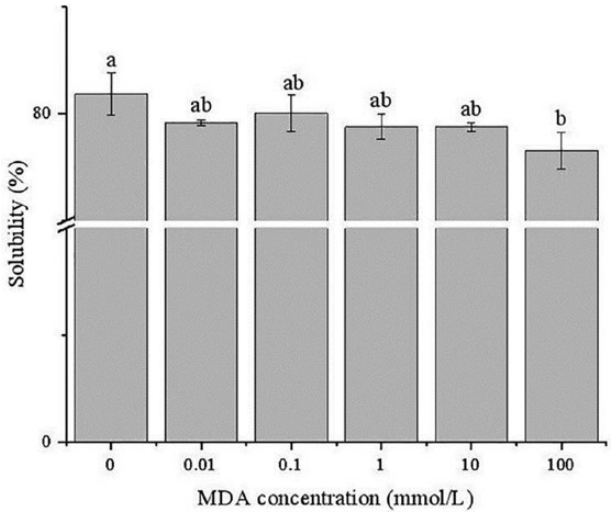

Figure 1. Effect of oxidation on solubility of amandin.

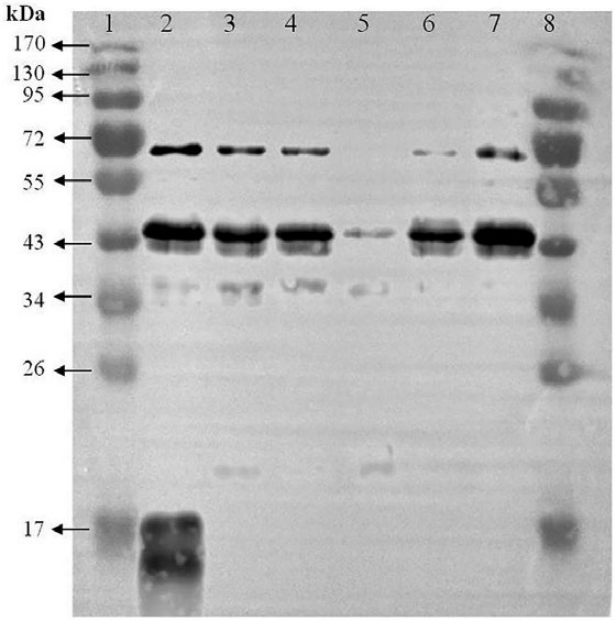

Figure 2. Western blot analysis of amandin with different oxidation levels. 1 and 8 were markers, and 2, 3, 4, 5, 6 and 7 were 0 mmol/L MDA, 0.01 mmol/L MDA, 0.1 mmol/L MDA, 1 mmol/L MDA, 10 mmol/L MDA, and 100 mmol/L MDA, respectively.

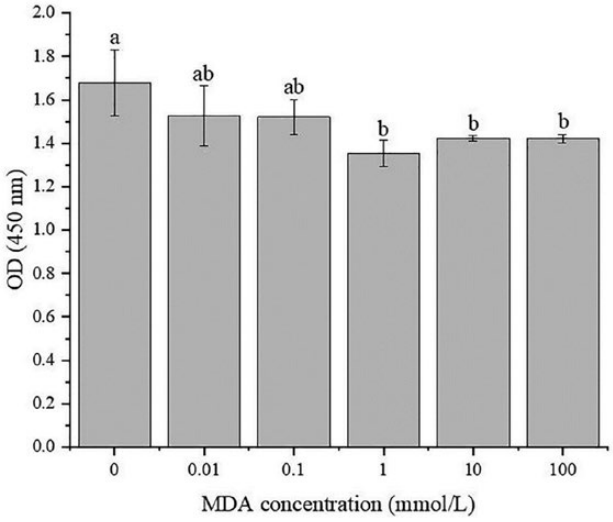

Figure 3. Effects of different concentrations of MDA on the IgG binding capacity of amandin.

Effects of oxidation on immunoreactivity of amandin

Western blotting

Oxidation changed the structure of amandin, leading to changes in conformational epitopes of amandin, which affected its immunoreactivity. As shown in Figure 2, the 70, 43, and 17 kDa bands of amandin could bind to rabbit IgE, suggesting that amandin had a certain potential immunoreactivity. When the concentration of MDA increased to 0.1 mmol/L, the bands at 70 kDa and 43 kDa became slightly lighter, the bands around 17 kDa disappeared, and the bands at around 34 kDa became darker. These results indicated that mild oxidation opened the protein structure and might destroy the conformational epitopes of higher molecular weight band, but also increased some conformational epitopes of the lower molecular weight band. When MDA concentration was 1 mmol/L, the bands at 70 kDa disappeared, and the bands at 43 kDa and 34 kDa became significantly lighter. The IgE-binding ability of amandin was the lowest, indicating that amandin oxidized by 1 mmol/L MDA had the lowest potential allergenicity. With a further increase of the MDA concentration, the band at around 70 kDa reappeared and gradually became darker, and the band at 43 kDa became obviously darker, while the band at around 34 kDa disappeared. The phenomenon suggested that a high degree of oxidation leads to protein rearrangement and then aggregation through disulfide bonds, hydrophobic interactions and electrostatic interactions, resulting in the destruction of part of the conformational epitopes. The results were consistent with the change trend of the corresponding bands in SDS-PAGE (Figure S1). Liu *et al.* (2021b) investigated the effects of dielectric barrier discharge plasma treatment on the structure and immunoreactivity of soybean glycinin. These results revealed conformational changes caused by oxidation of the amino group of the peptide bond within soybean glycinin and oxidation of tryptophan, tyrosine, and phenylalanine residues, which resulted in a significant decrease in the IgG/IgE binding capacity of soybean glycinin.

Almond ELISA kit

The immunoreactivity of oxidized amandin was quantitatively studied by almond ELISA kit. As the degree of oxidation increased, the immunoreactivity of amandin decreased significantly (Figure 3). Among them, the immunoreactivity of amandin treated with 1 mmol/L MDA was significantly reduced, which was 19.36% lower than that of untreated amandin. This was consistent with the western blotting results. Song *et al.* (2015) found an increase in carbonyl content, a decrease in free amino content and effective lysine content, and protein cross-linking in shrimp promyosin after MDA treatment. These structural changes might result in reduced immunoreactivity of shrimp promyosin. In addition, Lv *et al.* (2019) also found that oxidative induction of AAPH to shrimp proto-myoglobin produced corresponding structural changes that reduced its allergenicity. In conjunction with the study by Luo *et al.* (2022), MDA treatment led to an increase in the carbonyl content, cross-linking and aggregation of amandin, and a significant decrease in the content of amino acids (serine, glutamic acid, and lysine *et al.*) of amandin (Huang *et al.*, 2017). The immunoreactivity of proteins is related to changes in protein conformation. These conformational changes of amandin resulted in a significant reduction in immunoreactivity. The expansion and aggregation of protein structure might bury or destroy the inherent conformational epitopes, and the changes in active amino acids in MDA treated proteins might affect the inherent linear epitopes.

Changes in immunoreactivity during amandin digestion

SDS-PAGE analysis

Proteins were broken down into small peptides by pepsin by acting on phenylalanine, tyrosine, glutamic acid, and aspartic acid. Trypsin hydrolyzes peptide bonds in proteins made up of lysine or arginine carboxyl groups and amino groups of

other amino acids to hydrolyze proteins into small-molecule peptides to promote absorption (Xiang *et al.*, 2020). Figure 4 shows the SDS-PAGE of the digestion process of amandin in SGF. The 0 min sample was the amandin in SGF without pepsin. With the prolongation of digestion time, the digestibility of different molecular weight bands of amandin was significantly different. The bands at 70 kDa and 43 kDa disappeared after 30 min of digestion. A new band (31 kDa) appeared after 5 min of digestion, and then disappeared after 30 min of digestion. This might be due to the degradation of the bands at 70 kDa and 43 kDa. After 60 min of digestion, there were only 21 kDa and 14.4 kDa bands. The results were consistent with those of amandin digestion by Toomer *et al.* (2013). SDS-PAGE profiles of amandin (Figure S1) with different oxidation levels under SGF digestion were compared and analyzed. The results indicated that the degradation rate of amandin with 0.01–0.1 mmol/L MDA was basically the same during SGF. However, amandin oxidized by 1 mmol/L MDA was digested relatively quickly in SGF. The bands at around 70 kDa and 43 kDa disappeared at 5 min, the bands at 24 kDa vanished at 10 min, and the bands at 26 kDa did not disappear until 90 min. With increasing MDA concentration (10–100 mmol/L), the degradation rate of amandin during SGF slowed down. Li *et al.* (2020) found that the molecular weight of the seed kernel protein induced by AAPH increased gradually in SGF digestion. This was because with the increase of oxidation degree, protein cross-linked aggregation occurred and covered the cleavage site of pepsin, thus affecting protein digestibility, which was consistent with the trend of SGF digestion results in this study. The aggregation and cross-linking of amandin occurred after treatment with MDA (10–100 mmol/L), which masked the recognition sites of digesting proteases (pepsin and intestinal protease) and delayed its digestion in SGF. Figure 5 shows the SDS-PAGE profiles of amandin digestion in SIF. After trypsin digestion, amandin treated with 0–0.01 mmol/L MDA had only 14.4 kDa peptide, while amandin induced by MDA oxidation above 0.1 mmol/L still

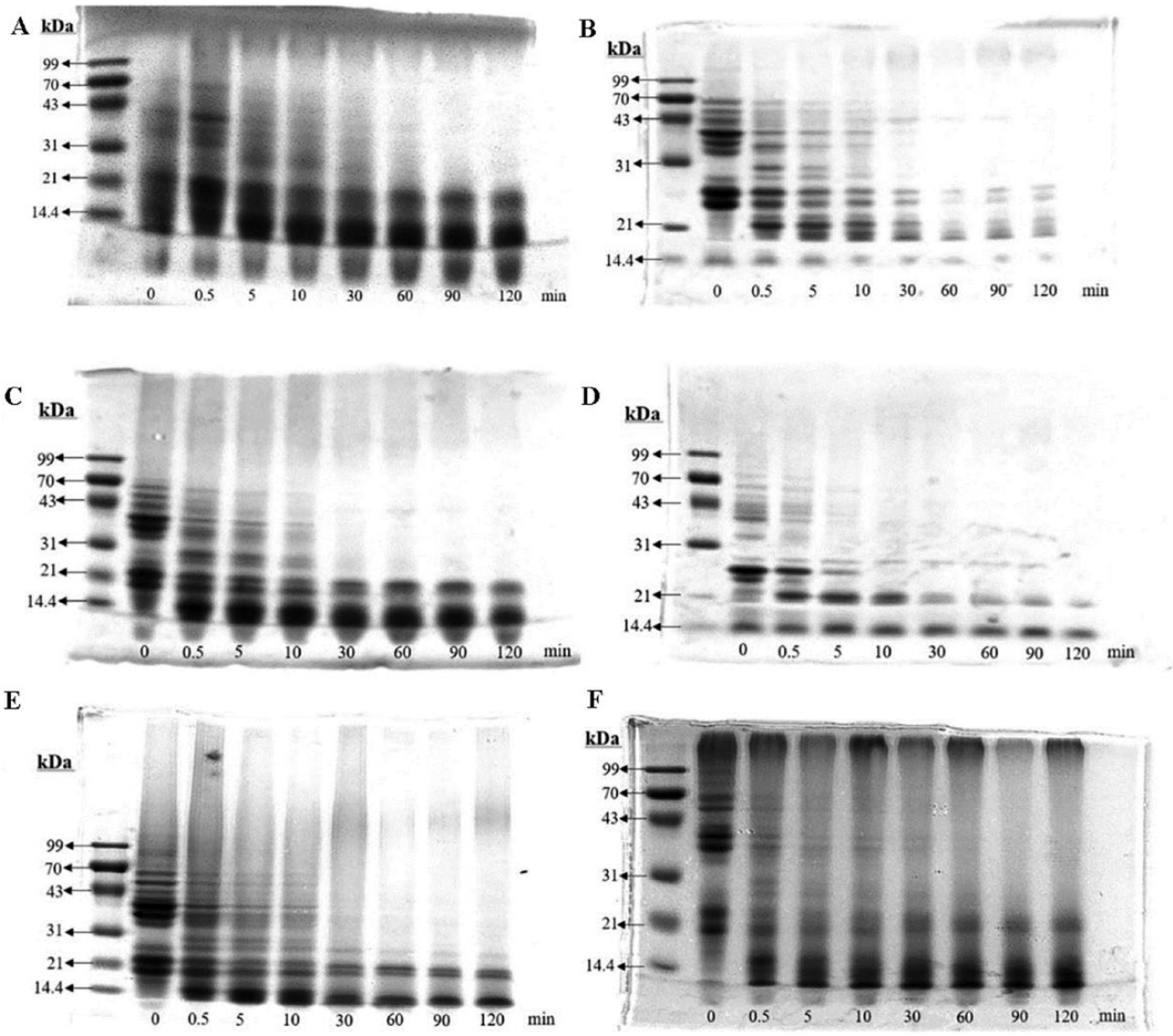

Figure 4. SDS-PAGE profile of amandin with different oxidation levels to SGF, in which A, B, C, D, E, and F were treated with 0 mmol/L MDA, 0.01 mmol/L MDA, 0.1 mmol/L MDA, 1 mmol/L MDA, 10 mmol/L MDA, and 100 mmol/L MDA, respectively.

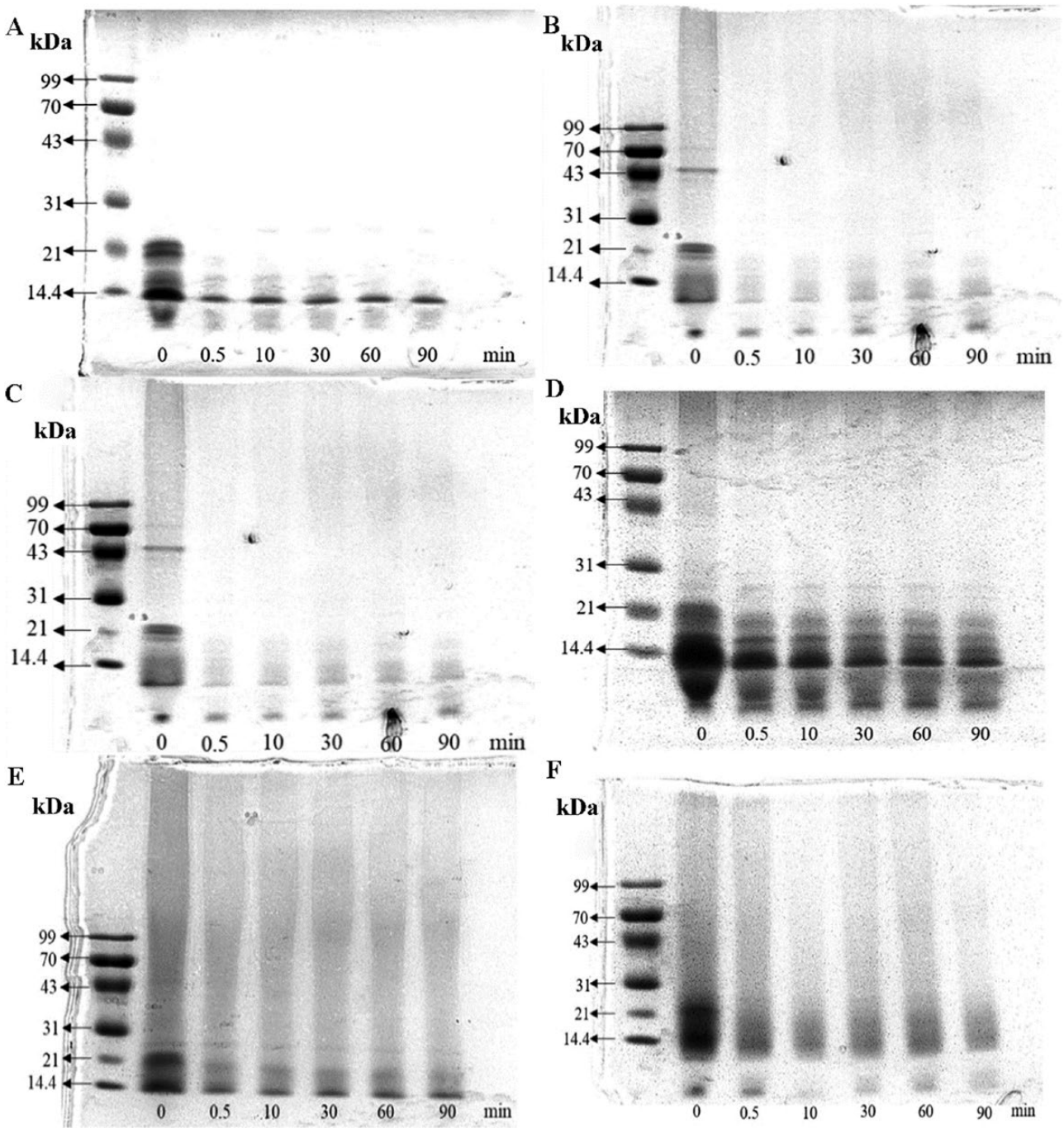

Figure 5. SDS-PAGE profile of amandin with different oxidation levels to SIF, in which A, B, C, D, E, and F were treated with 0 mmol/L MDA, 0.01 mmol/L MDA, 0.1 mmol/L MDA, 1 mmol/L MDA, 10 mmol/L MDA, and 100 mmol/L MDA, respectively.

had 21 kDa peptide. Intestinal digestion time had little effect on proteolysis.

Western blotting

After oxidation, amandin could resist pepsin digestion, prolong the residence time in SGF, and increase the possibility of transfer to jejunum mucosa for absorption (Toomer *et al.*, 2013). There were significant differences in the IgG binding capacity of amandin with different levels of oxidation in the process of SGF digestion (Figure 6). In the process of trypsin digestion, no other bands binding to rabbit IgG were observed, except for 0–0.01 mmol/L MDA treatment of amandin, the band at around 17 kDa was bound to rabbit IgG (Figure 7). As the MDA concentration increased, amandin showed immunoreactivity for a longer time during SGF digestion. The peptide without binding to rabbit IgG was observed before 5 min of digestion. This might be because the pH of the SGF was approximately 2.0, which had a certain impact on the structure of amandin, thereby affecting its ability to bind to rabbit IgG. Sun *et al.* (2020) found that low pH incubation could reduce the IgG binding capacity of black kidney bean lectin. Low pH induced protein unfolding, and pH transfer

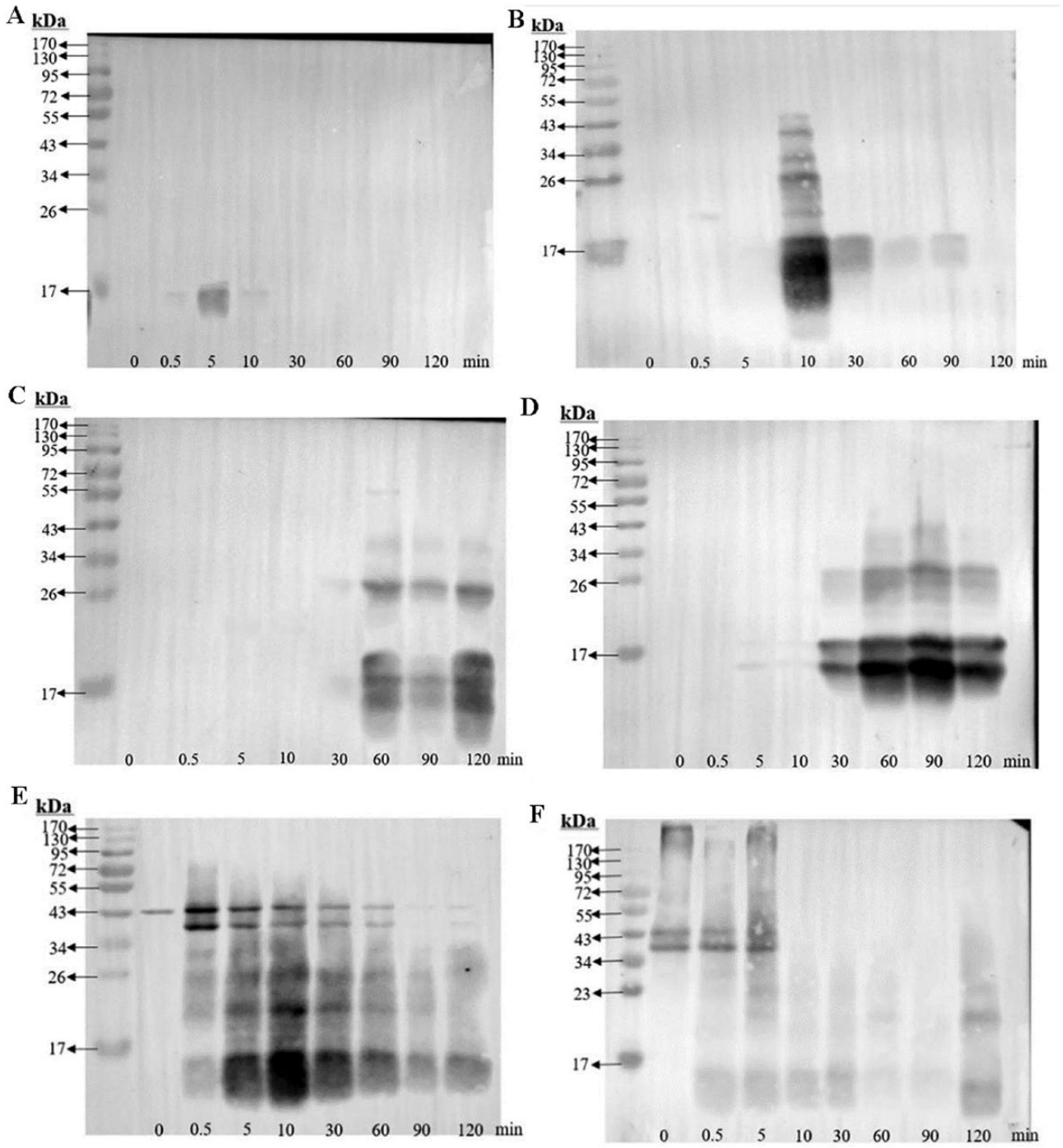

Figure 6. Western blot profile of amandin with different oxidation levels to SGF, in which A, B, C, D, E, and F were treated with 0 mmol/L MDA, 0.01 mmol/L MDA, 0.1 mmol/L MDA, 1 mmol/L MDA, 10 mmol/L MDA, and 100 mmol/L MDA, respectively. PVDV membrane of Western blot presents the profile of amandin at different oxidation levels to SGF.

treatment resulted in limited structural rearrangement that reduced IgG binding capacity. When the concentration of MDA was 0.01–1 mmol/L, amandin did not bind to rabbit IgG in the early stage of digestion (0–5 min), but it bound to rabbit IgG in the middle and late stages of digestion (10–120 min). This was not only because the digestion process might expose the antigenic determinants within the protein, but also because peptide bonds might break during hydrolysis, leading to the formation of new epitopes (Czubinski *et al.*, 2017). When the oxidation degree was high (10–100 mmol/L MDA), amandin cross-linked and aggregated, and the speed of gastric digestion was slow. The whole process of gastric digestion has immunoreactivity.

Almond ELISA kit

With the extension of simulated digestion time, the immunoreactivity of amandin digestive solution decreased significantly (Figures 8 and 9). The immunoreactivity of amandin treated with 100 mmol/L MDA was higher than that treated with other concentrations during the whole digestive process of

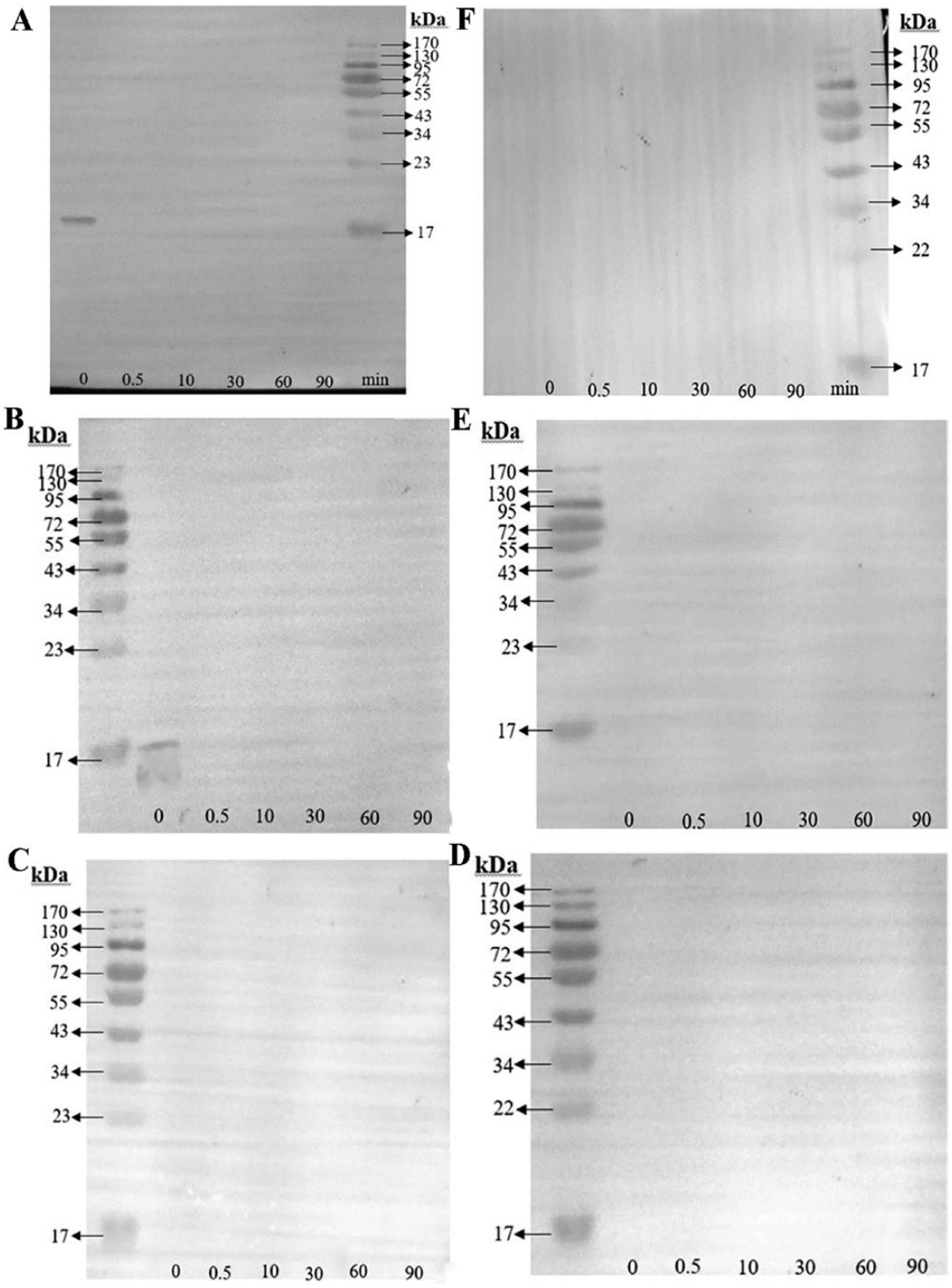

Figure 7. Western blot profile of amandin with different oxidation levels to SIF, in which A, B, C, D, E, and F were treated with 0 mmol/L MDA, 0.01 mmol/L MDA, 0.1 mmol/L MDA, 1 mmol/L MDA, 10 mmol/L MDA, and 100 mmol/L MDA, respectively. PVDV membrane of Western blot presents the profile of amandin at different oxidation levels to SIF.

SGF. Compared with SDS-PAGE profiles (Figure 4), it was further demonstrated that cross-linking or aggregation of proteins would cover the pepsin recognition site and delay protein digestion, resulting in the prolonged existence of immunoreactivity of amandin in SGF. ELISA kit data showed that immunoreactivity of amandin in SGF at different oxidation levels (0 min) was lower than that of amandin without simulated digestion (Figure 3). The result was consistent with western blotting analysis of SGF digestion (Figure 6), indicating that extreme pH had a certain influence on the immunoreactivity of amandin.

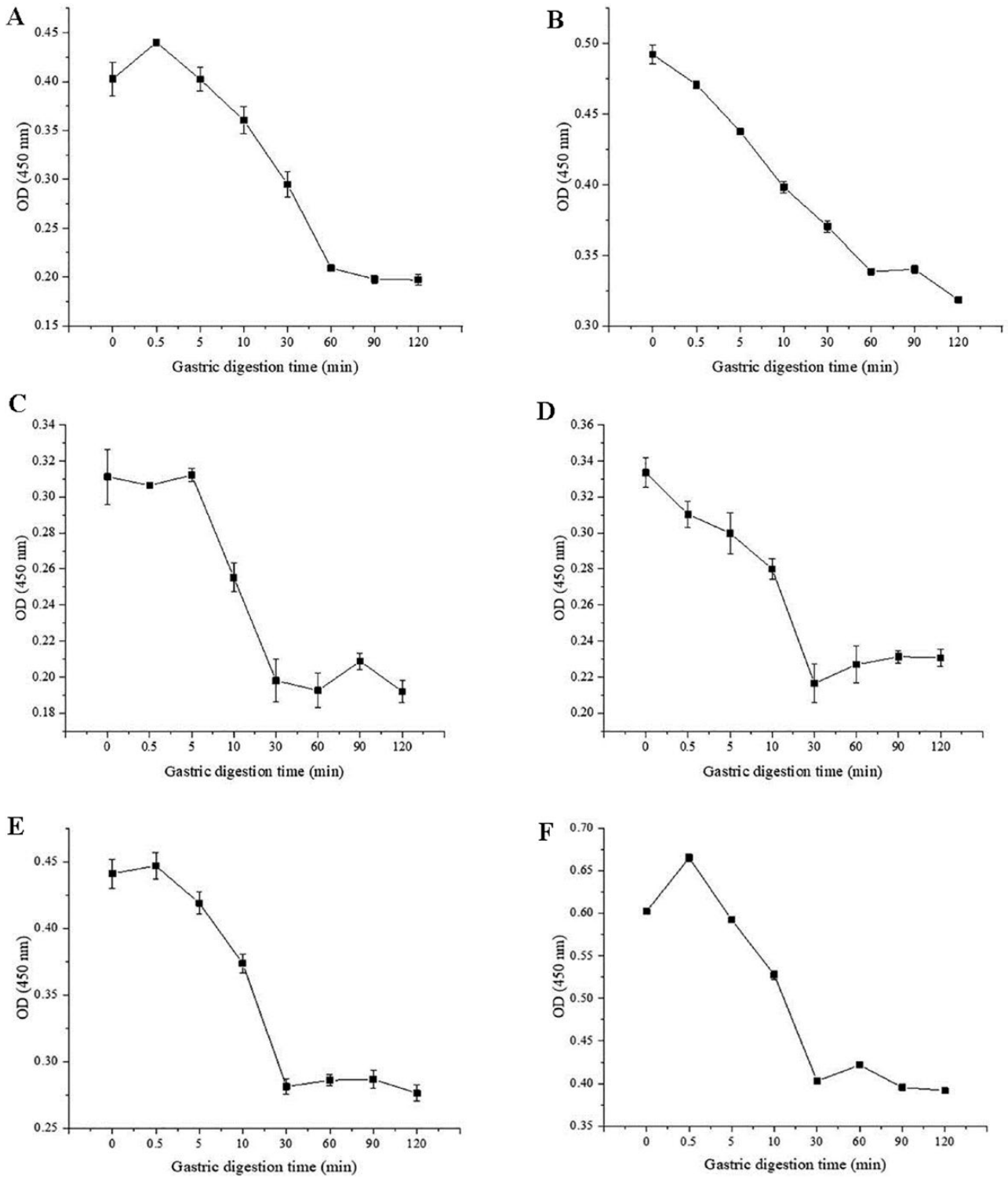

Figure 8. ELISA data of SGF digestion of amandin with different oxidation levels, in which A, B, C, D, E, and F were treated with 0 mmol/L MDA, 0.01 mmol/L MDA, 0.1 mmol/L MDA, 1 mmol/L MDA, 10 mmol/L MDA, and 100 mmol/L MDA, respectively.

LC-MS/MS analysis

According to the results of LC-MS/MS (Table 1), the extracted amandin mainly contained Pru du 6 (amandin), Gamma Conglutin 1 and TLP (Pru du 2). Pru du 6, a widely studied allergen in almonds, is an 11S almond seed storage protein that accounts for 60% of almond soluble protein (Youle and Huang, 1981). Two subunits of the hexamer protein Pru du 6 were isolated and sequenced, named Pru 1 and Pru 2, respectively. It can be precipitated from solution to microcrystals by lowering temperature or salt concentration (Zhang and Jin, 2020). Gamma conglutin 1, listed as 7S vicilin storage protein, is a sulfur-rich seed storage protein and an almond allergen (45 kDa IgE binding protein) (Mandalari and Mackie, 2018). TLP is a protein produced by many plants when they are

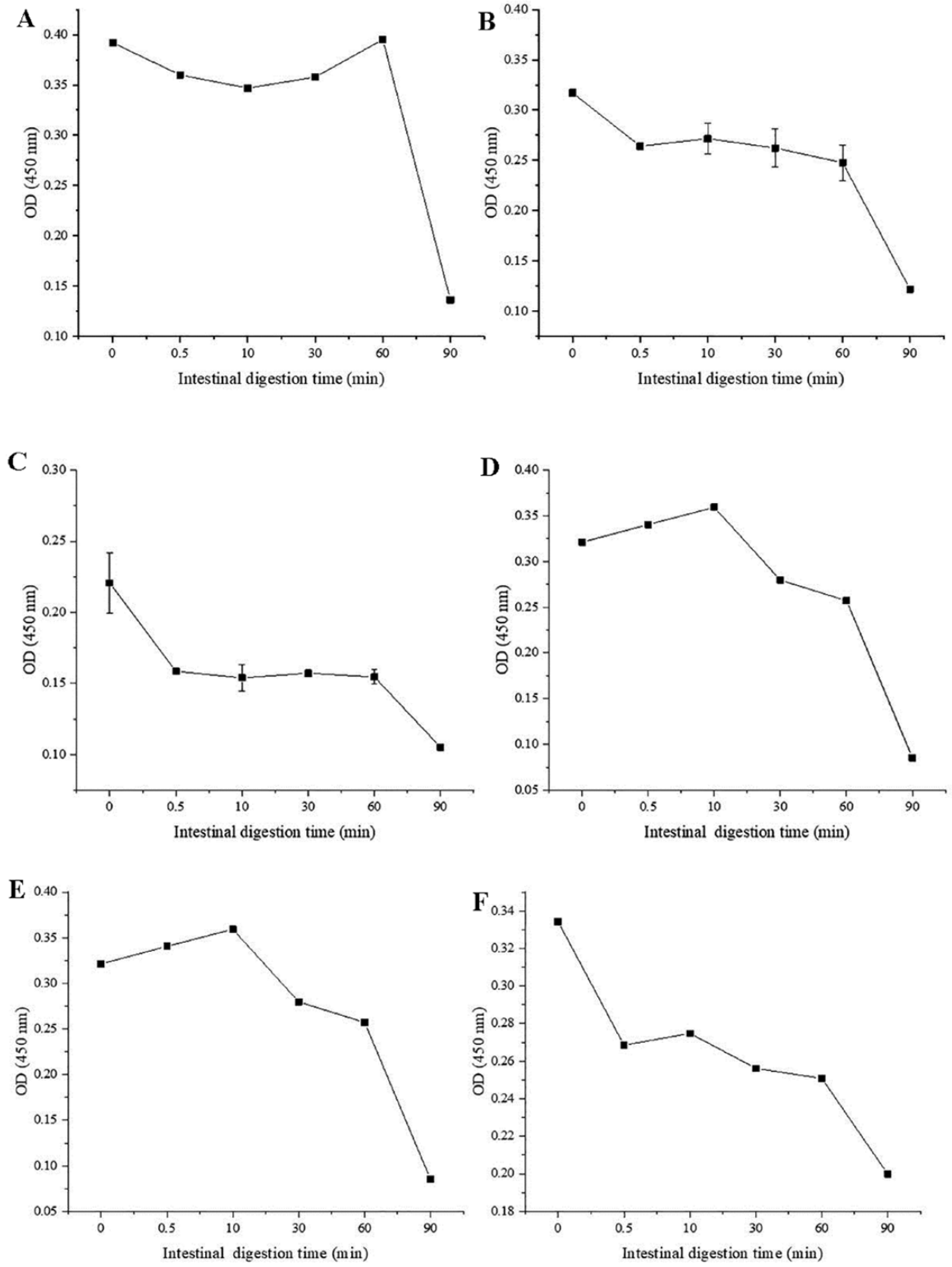

Figure 9. ELISA data of SIF digestion of amandin with different oxidation levels, in which A, B, C, D, E, and F were treated with 0 mmol/L MDA, 0.01 mmol/L MDA, 0.1 mmol/L MDA, 1 mmol/L MDA, 10 mmol/L MDA, and 100 mmol/L MDA, respectively.

stressed and is thought to be an almond allergen. However, the immunological characteristics of both Gamma Conglutin 1 and TLP need further study (Zhang and Jin, 2020).

At present, Willison *et al.* (2011) sorted out the known linear epitopes of amandin allergens and compared the detected amandin peptide sequences with them. The linear epitopes contained in amandin were found as shown in Figure 10. Fifteen peptides containing linear epitopes were detected in unoxidized amandin. The fewest linear epitopes were detected in amandin treated with 1 mmol/L MDA, and seven peptides

contained linear epitopes. The linear epitopes of 18 peptides were observed in 100 mmol/L MDA-treated amandin. The immunoreactivity of amandin treated with 1 mmol/L MDA was the lowest. Huang *et al.* (2017) pointed out that the high immunoreactivity of total hordein was attributed to the presence of cysteine residues in B-hordein, which could consume some formed hydroxyl radicals and protect C-hordein from attack. The immunoreactivity of hordein isolate treated by metal oxidation system was retained by approximately 30%, while C-hordein was retained by only 5% in the sandwich ELISA, probably due to the degradation of C-hordein in hordein and the cleavage of peptides or protein fragments on a large number of proline residues. The immunoreactivity was mainly a combination of linear and conformational epitopes. Combined with immunoreactivity data analysis (western blotting and ELISA), the immunoreactivity of amandin

Table 1. Proteins in amandin with different oxidation degrees were identified by LC-MS/MS

Accession	Description	MW (kDa)	Sequence coverage (%)		
			0 mmol/L MDA	1 mmol/L MDA	100 mmol/L MDA
E3SH28	Prunin 1 Pru du 6.0101	63.0	66.5±2.7[a]	54.7±2.2[b]	71.6±0.9[a]
Q43607	Prunin 1 Pru du 6	62.9	69.6±4.7[a]	52.8±1.3[b]	63.6±3.5[ab]
E3SH29	Prunin 2	56.9	66.0±1.3[b]	58.5±0.3[c]	71.3±2.5[a]
P82952	Gamma conglutin 1	46.9	52.9±2.0[b]	58.2±0.3[a]	21.0±1.8[c]

Data are expressed as the mean±SD from triplicate determinations. Different lowercase letters in the same column indicate significant differences ($P<0.05$; $n=3$).

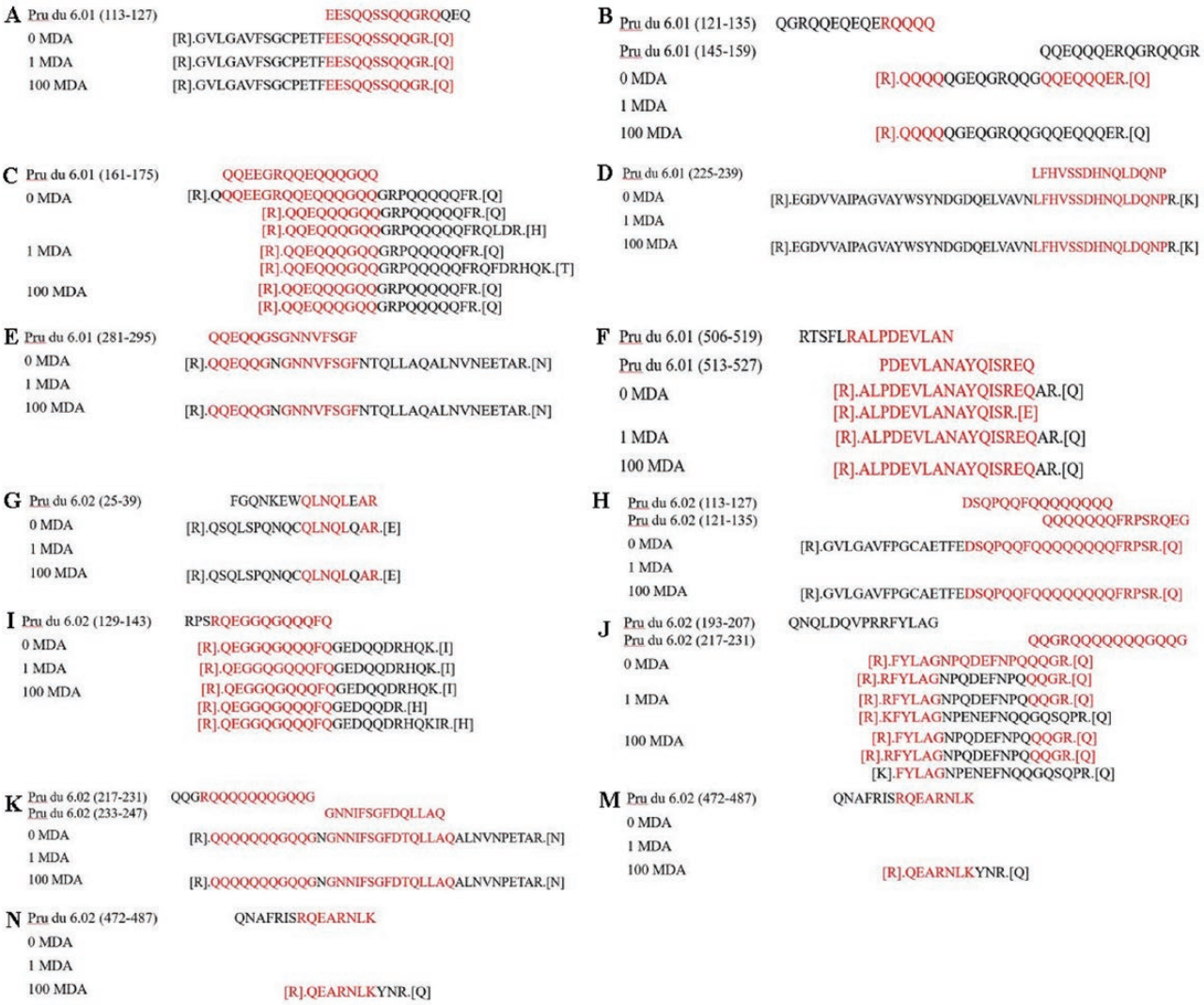

Figure 10. Comparisons of the peptides containing epitopes and the reported amandin allergenic epitopes.

treated with 1 mmol/L and 100 mmol/L MDA was significantly lower than that of untreated amandin. The reduction in immunoreactivity of amandin treated with 1 mmol/L MDA may be mainly due to the reduction of linear epitopes in amandin due to the cleavage of linear epitopes and oxidation of active amino acids. The linear epitopes of amandin were more abundant than those of amandin in 100 mmol/L MDA treatment, but their immunoreactivity was significantly

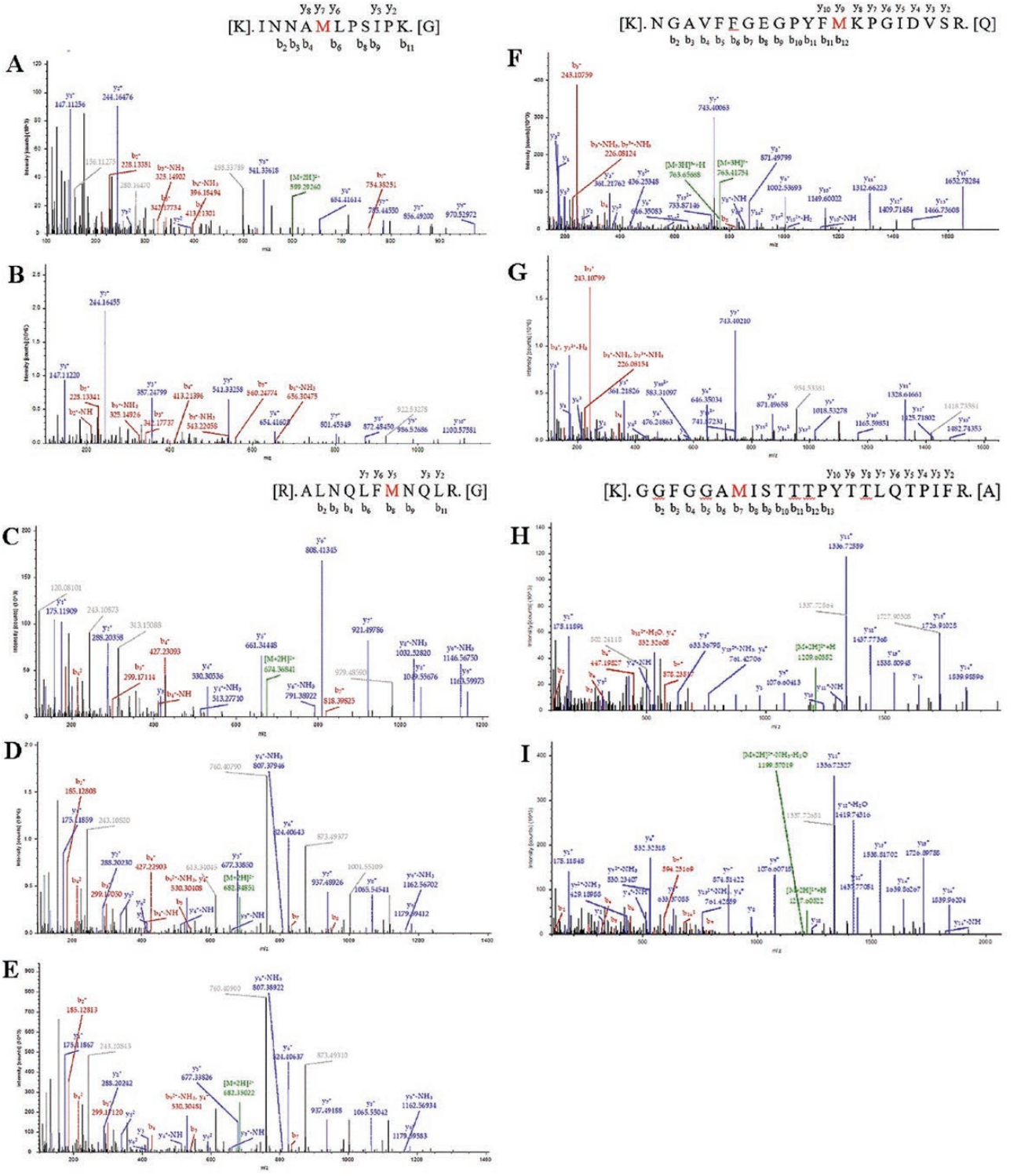

Figure 11. LC-MS/MS spectroscopic ion spectra of amino acids of amandin polypeptide. Y fragment ions are marked in blue and B fragment ions are marked in red. (A) and (B) are the ion spectra of peptide AA 264–274 in Gamma Conglutin 1 treated with 0 mmol/L MDA and 1 mmol/L MDA, respectively, in which M7 is oxidized to methionine sulfoxide. (C), (D), and (E) are the ion spectra of peptide AA 298–308 in Gamma Conglutin 1 treated with 0 mmol/L MDA, 1 mmol/L MDA, and 100 mmol/L MDA, respectively, in which M5 is oxidized to methionine sulfoxide. (F) and (G) are the ion spectra of peptide AA 220–240 in Gamma Conglutin 1 treated with 0 mmol/L MDA and 1 mmol/L MDA, respectively, in which M9 is oxidized to methionine sulfoxide. (H) and (I) are the ion spectra of peptide AA 275–297 in Gamma Conglutin 1 treated with 0 mmol/L MDA and 1 mmol/L MDA, respectively, in which M17 is oxidized to methionine sulfoxide.

reduced compared with that of amandin. Amandin aggregation was induced by 100 mmol/L MDA treatment, and its solubility was significantly reduced (Chhabra *et al.*, 2017). In conclusion, the destruction or burial of conformational epitopes was dominant in amandin treated with 100 mmol/L MDA compared with the increase of linear epitopes; thus, its immunoreactivity was significantly reduced.

An oxygen atom was added when the methionine side chain was oxidized to sulfoxide. Each oxidized methionine had an increased mass residue of 16 Da, so this had been used for mass spectrometry analysis to identify methionine oxidation sites (Wagner and Fraser, 1987). The increase of peptide mass, combined with spectral counts of oxidized and non-oxidized peptides, could generally be used to estimate the degree of methionine oxidation (Lu *et al.*, 2018). A total of 87 trypsin digestion peptides, including four methionine oxidation peptides, were detected in amandin. In addition to methionine residues, peptides containing other oxidable amino acids such as histidine, tryptophan, γ-glutamic acid hemialdehyde, or 2-*oxo*-histidine could also show a mass shift Δm=+16.0 Da (Wüst and Pischetsrieder, 2016). However, the location of methionine sulfoxide in amino acid sequence could be determined from Figure 11. [K].INNAMLPSIPK.[G], corresponding to the residues of Gamma Conglutin 1 264–274. The MS/MS map of the peptide showed that the mass of *y* (7) after oxidation of 1 mmol/L MDA was 801.45349, with a mass modification of 16 amu compared with that of the unoxidized peptide (785.44550). [R].ALNQLFMNQLR.[G] is the 298–308 residue of Gamma Conglutin 1. The MS/MS map of the peptide showed that the *y* (5) mass after oxidation of 1 mmol/L MDA and 100 mmol/L MDA was 677.33850 and 677.33826, respectively. Compared with the unoxidized mass (661.34448), the *y* (5) mass was modified by 16 amu. [K].NGAVFFGEGPYFMKPGIDVSR.[Q] corresponded to the 220–240 residues of Gamma Conglutin 1. The MS/MS map of the peptide showed that the *y* (9) mass of 1 mmol/L MDA oxidized was 1018.53278, and there was 16 amu modification compared with that of the unoxidized mass (1002.53693). Peptides [K].GGFGGAMISTTTPYTTLQTPIFR.[A] corresponded to Gamma Conglutin 1 residues 275–297. The MS/MS map of the peptide showed that the *b* (7) mass after oxidation of 1 mmol/L MDA was 594.23169, respectively, and there was 16 amu modification compared with the unoxidized mass (578.23517). The oxidation of amino acids such as methionine was affected by adjacent amino acids. Methionine surrounded by acidic amino acids, such as aspartic acid (D) and glutamic acid (E), or by alanine (A), threonine (T) and serine (S), was more easily oxidized (Jeong *et al.*, 2016). There was A near the methionine in the peptides [K].INNAMLPSIPK.[G] and [K].GGFGGAMISTTTPYTTLQTPIFR.[A]. The content of Gamma Conglutin 1 was the highest in the extracted amandin, and all identified peptides with methionine sulfoxide also belonged to Gamma Conglutin 1. These results suggested that Gamma Conglutin 1 was more susceptible to oxidation of methionine than other identified proteins, thereby reducing its nutritional value. This might be because Gamma Conglutin 1 is a sulfur-rich seed storage protein. Protein sulfhydryl groups are sensitive to protein oxidation. Under different oxidation conditions and different oxidation intensities, protein sulfhydryl groups might undergo reversible oxidation to form disulfide bonds and sulfonic acid. Irreversible oxidation to sulfur-containing compounds with non-disulfide bonds might also occur. MDA is the main secondary product of lipid oxidation and can form stable adducts with sulfhydryl groups (Xin *et al.*, 2022).

Conclusions

In this study, SDS-PAGE, western blotting, and ELISA tests were performed to investigate the immunoreactivity effects of oxidation on amandin and its digestion process. Furthermore, the changes in the oxidation sites and linear epitopes of amandin during the oxidation process were studied by LC-MS/MS. The immunoreactivity of amandin was significantly reduced by both 1 mmol/L and 100 mmol/L MDA treatment, but the reasons for the reduction in immunoreactivity were different. Oxidation might lead to cross-linking and aggregation of amandin, obscuring protease recognition sites and reducing protein digestion in the gastrointestinal tract. It could also affect the immunoreactivity of proteins by changing the conformational and linear epitopes of amandin. LC-MS/MS also identified the protein sites in amandin that were easily oxidized. In this paper, the effect of oxidation on the immunoreactivity of amandin was studied, and the oxidation sites of amandin induced by MDA were further explored. This enabled us to understand the structure and immunoreactivity changes in amandin oxidation induced by lipid peroxidation, thus revealing the mechanism of immunoreactivity changes during the production, processing and storage of amandin.

Supplementary Material

Supplementary material is available at *Food Quality and Safety* online.

Funding

This study was financially supported by from the National Natural Science Foundation of China (No. 31860431).

Conflict of interest

The authors declared that they have no conflicts of interest to this work.

References

Chhabra, G. S., Liu, C., Su, M., *et al.* (2017). Effects of the Maillard reaction on the immunoreactivity of amandin in food matrices. *Journal of Food Science*, 82: 2495–2503.

Costa, J., Mafra, I. (2022). Rosaceae food allergy: A review. *Critical Reviews in Food Science and Nutrition*, 62(1): 1–38.

Czubinski, J., Montowska, M., Springer, E., *et al.* (2017). Immunoreactivity changes during lupin seed storage proteins digestion. *European Food Research and Technology*, 243(12): 2095–2103.

Gazme, B., Rezaei, K., Udenigwe, C. C. (2022). Epitope mapping and the effects of various factors on the immunoreactivity of main allergens in egg white. *Food & Function*, 13(1): 38–51.

Huang, X., Sontag-Strohm, T., Stoddard, F. L., *et al.* (2017). Oxidation of proline decreases immunoreactivity and alters structure of barley prolamin. *Food Chemistry*, 214: 597–605.

Huang, Q., Huang, X., Liu, L., *et al.* (2021a). Effect of nano eggshell calcium on the structure, physicochemical, and gel properties of threadfin bream (*Nemipterus virgatus*) actomyosin. *LWT-Food Science and Technology*, 150: 112047.

Huang, Q., Liu, L., Wu, Y., *et al*. (2021b). Mechanism of differences in characteristics of thick/thin egg whites during storage: Physicochemical, functional and molecular structure characteristics analysis. *Food chemistry*, 369: 130828.

Huang, X., Sun, L., Liu, L., *et al*. (2022). Study on the mechanism of mulberry polyphenols inhibiting oxidation of beef myofibrillar protein. *Food Chemistry*, 372: 131241131241.

Jeong, J. Y., Jung, E. Y., Jeong, T. C., *et al*. (2016). Analysis of methionine oxidation in myosin isoforms in porcine skeletal muscle by LC-MS/MS analysis. *Korean Journal for Food Science of Animal Resources*, 36(2): 254–261.

Li, S., Li, Z., Li, X., *et al*. (2020). Effect of AAPH oxidation on digestion characteristics of seed watermelon (*Citrullus lanatus* var) kernels protein isolates. *Food Science and Human Wellness*, 9(4): 402–410.

Li, F., Wu, X., Wu, W. (2021). Effects of protein oxidation induced by rice bran rancidity on the structure and functionality of rice bran glutelin. *LWT-Food Science and Technology*, 149: 111874.

Liu, C. Y., Guo, S. D., Yu, J. Z., *et al*. (2015). Fasudil mediates cell therapy of EAE by immunomodulating encephalomyelitic T cells and macrophages. *European Journal of Immunology*, 45(1): 142–152.

Liu, X., Wang, J., Liu, L., *et al*. (2021a). Quantitative *N*-glycoproteomic analyses provide insights into the effects of thermal processes on egg white functional properties. *Food Chemistry*, 342: 128252.

Liu, Z. W., Zhou, Y. X., Wang, F., *et al*. (2021b). Oxidation induced by dielectric barrier discharge (DBD) plasma treatment reduces IgG/IgE binding capacity and improves the functionality of glycinin. *Food Chemistry*, 363: 130300.

Lu, H., Luo, Y., Lametsch, R. (2018). Proteomic profiling of oxidized cysteine and methionine residues by hydroxyl radicals in myosin of pork. *Food Chemistry*, 243: 277–284.

Luo, X., Wang, Q., Wu, Y. Y., *et al*. (2022). Mechanism of effect of heating temperature on functional characteristics of thick egg white. *LWT-Food Science and Technology*, 154.

Lv, L., Lin, H., Li, Z., *et al*. (2017). Determining the effect of malondialdehyde on the IgE-binding capacity of shrimp tropomyosin upon *in vitro* digestion. *Journal of the Science of Food and Agriculture*, 97: 4588–4594.

Lv, L., Lin, H., Li, Z., *et al*. (2019). Structural changes of 2,2′-azobis(2-amidinopropane) dihydrochloride (AAPH) treated shrimp tropomyosin decrease allergenicity. *Food Chemistry*, 274: 547–557.

Mandalari, G., Mackie, A. (2018). Almond allergy: An overview on prevalence, thresholds, regulations and allergen detection. *Nutrients*, 10: 1706.

Roux, K. H., Teuber, S. S., Robotham, J. M., *et al*. (2001). Detection and stability of the major almond allergen in foods. *Journal of Agricultural & Food Chemistry*, 49(5): 2131–2136.

Song, Y., Li, Z., Lin, H., *et al*. (2015). Effect of malondialdehyde treatment on the IgE binding capacity and conformational structure of shrimp tropomyosin. *Food Chemistry*, 175: 374–380.

Su, M., Liu, C., Roux, K. H., *et al*. (2017). Effects of processing and storage on almond (*Prunus dulcis* L.) amandin immunoreactivity. *Food Research International*, 100: 87–95.

Sun, X., He, S., Ye, Y., *et al*. (2020). Combined effects of pH and thermal treatments on IgE-binding capacity and conformational structures of lectin from black kidney bean (*Phaseolus vulgaris* L.). *Food Chemistry*, 329: 127183.

Tiwari, R. S., Venkatachalam, M., Sharma, G. M., *et al*. (2010). Effect of food matrix on amandin, almond (*Prunus dulcis* L.) major protein, immunorecognition and recovery. *LWT-Food Science and Technology*, 43(4): 675–683.

Toomer, O. T., Do, A., Pereira, M., *et al*. (2013). Effect of simulated gastric and intestinal digestion on temporal stability and immunoreactivity of peanut, almond, and pine nut protein allergens. *Journal of Agricultural and Food Chemistry*, 61(24): 5903–5913.

Wagner, R. M., Fraser, B. A. (1987). Analysis of peptides containing oxidized methionine and/or tryptophan by fast atom bombardment mass spectrometry. *Biomedical & Environmental Mass Spectrometry*, 14(2): 69–72.

Wang, J., Xiao, J., Liu, X., *et al*. (2021). Tandem mass tag-labeled quantitative proteomic analysis of tenderloins between Tibetan and Yorkshire pigs. *Meat Science*, 172: 108343.

Willison, L., Tripathi, P., Sharma, G., *et al*. (2011). Cloning, expression and patient IgE reactivity of recombinant Pru du 6, an 11S globulin from almond. *International Archives of Allergy and Immunology*, 156: 267–281.

Wüst, J., Pischetsrieder, M. (2016). Methionine sulfoxide profiling of milk proteins to assess the influence of lipids on protein oxidation in milk. *Food & Function*, 7: 2526–2536.

Xiang, S., Zou, H., Liu, Y., *et al*. (2020). Effects of microwave heating on the protein structure, digestion properties and Maillard products of gluten. *Journal of Food Science and Technology*, 57(6): 2139–2149.

Xin, L., Zhang, Y., Duan, W., *et al*. (2022). Effect of malondialdehyde oxidation on structure and physicochemical properties of amandin. *International Journal of Food Science & Technology*, 57(5): 2646–2655.

Yang, R., Geng, F., Huang, X., *et al*. (2020). Integrated proteomic, phosphoproteomic and *N*-glycoproteomic analyses of chicken eggshell matrix. *Food Chemistry*, 330: 127167.

Youle, R. J., Huang, A. H. C. (1981). Occurrence of low molecular weight and high cysteine containing albumin storage proteins in oilseeds of diverse species. *American Journal of Botany*, 68(1): 44–48. .

Zaffran, V. D., Sathe, S. K. (2018). Immunoreactivity of biochemically purified amandin from thermally processed almonds (*Prunus dulcis* L.). *Journal of Food Science*, 83(7): 1805–1809.

Zhang, J. Q., Gao, S. X., Sheng, W., *et al*. (2013). Development of double-antibody sandwich ELISA for the detection of the almond allergen amandin. *Food Science*, 34(16): 173–177. (in Chinese)

Zhang, Y., Zhang, J., Sheng, W., *et al*. (2016). Effects of heat and high-pressure treatments on the solubility and immunoreactivity of almond proteins. *Food Chemistry*, 199: 856–861.

Zhang, Y., Jin, T. (2020). Almond allergens: update and perspective on identif ication and characterization. *Journal of the Science of Food and Agriculture*, 100(13): 4657–4663.

Zhou, L., Sun, Y., Wu, F. (2019). Effects of oxidation by malondialdehyde on the structure and function of rice bran protein. *Food Science*, 40(12): 98–107.